Kodaikanal Obs. Bull. Ser. A (1978) 2, 95-104.

REFLECTION NEBULA IN THE FAR-ULTRAVIOLET

1. Icy Grains

G. A. SHAH and K. S. KRISHNA SWAMY*

ABSTRACT

Some models of the reflection nebula in the form of homogeneous plane-parallel slab containing singly scattering dirty ice grains as test case have been given. The three geometric cases of the star behind, within and in front of the nebula have been considered. The size distribution of the grains has also been incorporated. We have calculated the nebular surface brightness and band integrated colours and polarization. The present results on the nebular surface brightness have been directly compared with the very recent far-ultraviolet observations of the Merope reflection nebula.

Key Words: reflection nebula– interstellar grains -far-ultraviolet colours and polarization

1. Introduction

The reflection nebulae provide an excellent opportunity for observations and the theoretical models in search for the nature of ubiquitous dust grains. The Merope reflection nebula is particularly well suited for the observations of surface brightness, colour differences and polarization as function of wavelength and offset angle. The earlier ground-based observations (Elvius and Hall, 1966; Greenberg and Roark, 1967) were confined to UBV photometry and polarimetry. The related theoretical models (Greenberg and Roark, 1967; Greenberg and Hanner, 1970; Shah, 1974) based on homogeneous plane-parallel slab containing single scattering grains have brought out certain trends of variation in the colours and polarization. However, it is known that the observations in the UV region can bring out characteristics of the grain properties which are not revealed in the visual region. This has been amply demonstrated from the far-ultraviolet extinction observations (Bless and Savage, 1972; Nandy *et al.* 1975). Therefore, it is of interest to calculate the expected nebular surface brightness, colours and polarizations of the scattered light in the ultraviolet region. Since the illuminating star in the Merope reflection nebula is of spectral class B6 IV, it is reasonable to ignore emission and ionization. It may be noted that a nebula usually has a composite spectrum if the spectral class of the illuminating star is B0-B1 or earlier (Kaplan and Pikelner, 1970).

Here we consider some simple models of reflection nebula based on plane-parallel slabs and single scattering. We have used dirty ice grains as a test case. The stellar energy distribution, measured wavelength-dependent refractive indices of ice, grain size distribution, Mie scattering process etc. have been used as basic input quantities. We have calculated the far-ultraviolet colours in a manner analogous to the case of UBV photometry. The calculated surface brightness distribution across the nebula has been compared with the recent observations of the surface brightness of the Merope nebula obtained by Andriesse *et al.* (1977) with the help of ultarviolet photometer on board the ANS satellite. In what follows we delineate the systematics of the general trends and relate them to the basic properties of the grains and geometries of the reflection nebula.

2. Theoretical Consideration and Geometrical Models

We have assumed the reflection nebula in the form of a plane-parallel slab perpendicular to the line joining the observer and the star. The nebula is divided into a number of elementary slabs. The three cases (1) star behind the nebula (SBN), (2) star within the nebula (SWN) and (3) star in front of the nebula (SFN) have been considered. The finite aperture of the telescope has been included in the theoretical formulation of the models. The number density of the grains has been assumed to be uniform throughout the nebular region of interest. The frequency of the wave

* Tata Institute of Fundamental Research, Colaba, Bombay

before and after the scattering process remains the same. The two states of polarization in the orthogonal reference planes have been treated separately. The empirical correction for the extinction of light within the nebula has been taken into account on the basis of observations (Peytremann and Davis, 1974). The stellar energy distribution for Merope (23 Tau, B6 IV) as given by Andriesse *et al.* (1977) has been adopted here. The intensity is obtained by integration with respect to the elementary scattering volumes along the line of sight and with respect to the size of the dust grains. We have also computed the band integrated quantities. The definitions of colours and polarization as usual are adopted from Greenberg and Roark (1967).

The symbols and notations have the following meaning:

D = the distance from the observer to the illuminating star,

T = the thickness of the nebula,

H = the perpendicular distance from the star to the front surface of the nebula,

ϕ = the offset angle,

β = semi-vertex angle of the telescope 0.0015 radian,

h = the distance of the bottom of a typical elementary slab from the observer,

$\Delta\Omega$ = the solid angle of the telescope $\pi \tan^2 \beta$

S = the location of the star,

O = the location of the observer,

λ = wavelength of light,

a = size of the grain,

a_n = parameter in the size distribution function,

$m(\lambda) = m'(\lambda) - i\, m''(\lambda)$ = index of refraction.

A possible consideration in the present study is to include a certain number of much smaller particles (size, $a \gtrsim 0.005\ \mu$m) which are needed to account for the shape of the far-ultraviolet extinction curve beyond $\lambda^{-1} \sim 7 \mu m^{-1}$ (see, for *e.g.*, Greenberg and Hong, 1974). It may be assumed that the small particles are continuously generated to compensate for the effects of radiation pressure and destruction. In order to assess the importance of such small particles one must estimate their optical thickness *vis-a-vis* the classical larger sized particles which are thought to contribute the visual extinction. Let the size parameters and the number densities be (a_1, n_{o1}) and (a_2, n_{o2}), respectively, for small and large categories of particles. Following Greenberg (1977), we assume that the total surface area (S_1) of small particles is two times larger than that (S_2) of larger particles. Choosing the normalized size distribution function in the form

$$n_i(a)da \sim (n_{oi}/a_i) \exp[-5(a/a_i)^3]da, \quad i = 1, 2.$$

It can be shown that

$$\frac{n_{o1}}{n_{o2}} = f\left(\frac{a_2}{a_1}\right)^2, \quad \text{where} \quad f = \frac{S_1}{S_2}.$$

For $a_1 \sim 0.005\ \mu$m, $a_2 \sim 0.5\ \mu$m and $f = 2$, the ratio of the grain number densities turns out to be $(n_{o1}/n_{o2}) \sim 2 \times 10^4$. The corresponding ratio of the optical thicknesses is given by

$$\frac{\tau_1}{\tau_2} = \left(\frac{n_{o1}}{n_{o2}}\right)\left(\frac{a_1}{a_2}\right)^2\left(\frac{Q_1}{Q_2}\right)$$

where Q_1 and Q_2 are the extinction efficiencies of the two types of particles. For dirty ice grains, wavelength $\lambda = 0.15\ \mu$m, and using the above quoted values of (n_{o1}/n_{o2}), a_1 and a_2, one obtains $(\tau_1/\tau_2) \lesssim 1/18$. This implies that the small particles cannot play significant role in modifying the colours and intensity distribution of the reflection nebula in the far-ultraviolet. Due to finite absorptivity, *i.e.* some imaginary component of the index of refraction in the far-ultraviolet, most of the extinction or optical thickness of the small particles is caused by absorption efficiency. In fact, the scattering efficiency of small absorbing particles is likely to be three or more orders of magnitude smaller as compared to the absorption efficiency. Therefore, one cannot expect the component of the very small grains to modify the degree of isotropy of the phase function which would be mainly determined by the classical grains. Similarly a large number of small absorbing particles in conjunction with large particles can reduce the average albedo considerably below unity. This is evident from a glance at the quantitative tables of scattering parameters (see, for *e.g.*, Isobe, 1975) for real materials with finite absorptivity.

A related question regarding the multiple scattering within the reflection nebula must now be examined in the light of far-ultraviolet optical thickness and albedo of the totality of the grains. According to Kaplan and Pikelner (1970), if the optical thickness $\tau \gtrsim 1$ and albedo of the grains is close to unity,

higher order scattering must be considered along with single scattering. These conditions are satisfied in dense dust cloud complexes such as, for example, globules or compact spherical nebula NGC 7023. Vanysek and Solc (1973) have used Monte Carlo technique to show that the multiple scattering can introduce depolarization effects in dense clouds. The depolarization factor is a function of the optical thickness. For instance, when τ increases from 0.4 to 1.5 the polarization is roughly halved for the same geometrical distance of the nebular region from the illuminating star.

We can make an estimate of the optical thickness of Merope reflection nebula by considering it as a 'Standard' cloud with gaseous particle densities in the range $3 \lesssim n_n(\mathrm{cm}^{-3}) \lesssim 10^3$ (Watson, 1975) From the observations including the ultraviolet extinction of variety of objects (see, *e.g.*, Lilley, 1955; O'Dell and Hubbard, 1965; O'Dell *et al*, 1966, Krishna Swamy and O'Dell, 1967; Isobe, 1971; Jenkins and Savage, 1974), one has the following relation between dust and gas concentrations :

$$(n_g \sigma_g / n_n) \simeq 10^{-21} \text{ cm}^2 \text{ per atom}$$

where n_g and σ_g are the number density and extinction cross-section, respectively, of the grains. This ratio is approximately independent of location in the galaxy (Aannestad and Purcell, 1973). Using the above quoted n_n and thickness of the Merope nebula $\sim$ 1 pc, one has

$$3 \gtrsim \tau \gtrsim 0.03.$$

Noting the constraint that $\tau \sim 3$ is the upper limit and because of the absorptivity in the far-ultraviolet, it appears that the scattering optical thickness would become considerably smaller than unity. As mentioned earlier the albedo is also smaller than 1. This is corroborated by the recent OAO measurements (Lillie and Witt, 1976) on diffuse galactic light in the ultraviolet which give albedo $\lesssim 0.6$. In summary then it may be stated that we do not envisage two primary conditions (*viz.* $\tau \gtrsim 1$ and albedo $\simeq 1$) to be satisfied strongly enough in the case of Merope reflection nebula to warrant the use of multiple scattering. According to the most recent observations by Jura (1977), the dust in sister nebula (Maia) towards 20 Tau is in front of the star and that the nebula is optically thin. He further mentions that it is quite possible that the cloud observed to lie in front of 20 Tau might lie behind 23 Tau (Merope) as well. Therefore, in the present work, we have assumed single and independent scattering to hold. This preserves the simplicity and continuity with the earlier equivalent models in the UBV (see, for *e.g.*, Greenberg and Roark, 1967; Shah, 1974, 1977a, b).

2.1 *Case I. Star behind the nebula (SBN)*

The present treatment is similar to that of Greenberg and Roark (1967). The main difference is that we have considered, for sake of generality, the exact scattering volume intercepted by the extension of the telescope and the elementary slab. The scattering centre within the elementary volume is located with reasonable symmetry and is specified explicitly Therefore, the analytical expressions are different for all the three cases. The relevant equations for SBN are given by Shah (1974) and will not be repeated here. The general expression for intensity given there holds also for the cases of SWN and SFN.

2.2 *Case II. Star within the nebula (SWN)*

Two subcases must be considered separately.

2.2.1 *IIa : (h + δ) > D*

Fig. 1a represents this case in a schematic way. The observer is viewing the nebular slab x_1 x_2 y_1 y_2 at an offset angle ϕ with respect to the observer-star direction OS. The extension of the telescope intersects the elementary slab L'N' LN in ellipses L'M'N' and LMN with their centres at C' and C, respectively. The points P' and P are along the axis of the telescope. The scattering centre within the elementary volume MN N'M' is located at the centre C'' of the ellipse L''M''N'' which divides this volume into two equal parts. We define δ to be the perpendicular distance between the elliptical cross-sections L''M''N'' and LMN. Some distances and angles have been denoted as follows :

$OC'' = l_1$, $SC'' = l_2$, $OL = h$,

$LL'' = \delta$, $P''C'' = \gamma$,

$\phi = \angle SOP$, $\alpha = \angle L_N SP''$

$\phi_1 = \angle POC$, $\alpha_1 = \angle P''SC''$.

The useful relations are given below :

$$h = (D - H) + (i - 1)\,\Delta Z, \qquad (1)$$

where $i = 1, N$ elementary slabs. The limits of integration with respect to Z will be from $(D - H)$ to $(D - H + T)$ which covers the thickness of the slab.

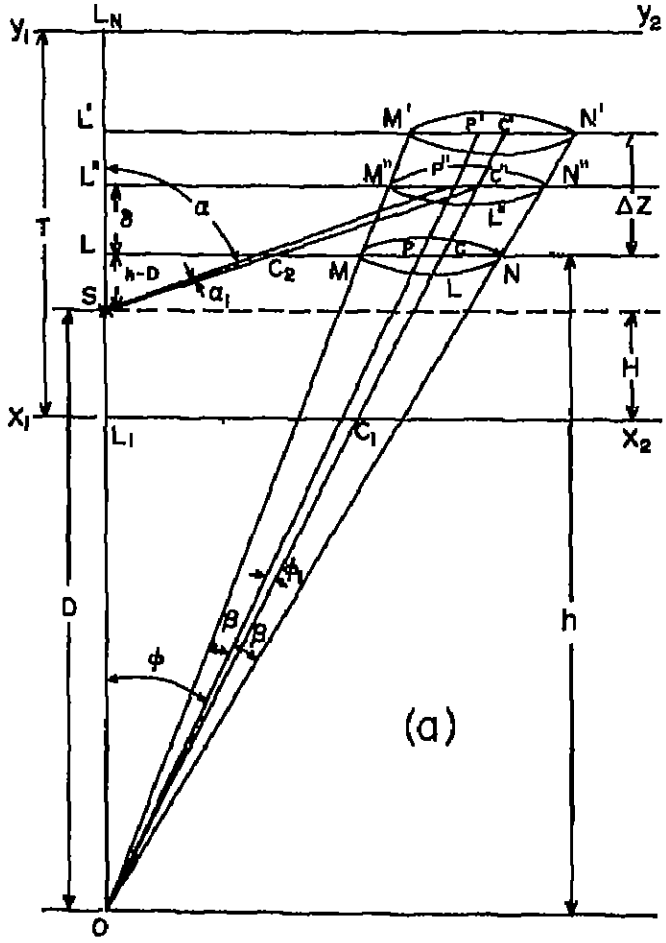

Fig. 1a. Schematic of the model reflection nebula in the form of homogeneous plane-parallel slab; (a) star within the nebula with the scattering centre more distant than the distance of the star from the observer, *i.e.* $h+\delta>D$.

This is best taken care of by using h as the variable for both the cases IIa and IIb.

$$\gamma = \frac{(h+\delta)\tan\phi\tan^2\beta}{\cos^2\phi - \sin^2\phi\tan^2\beta} \quad , \tag{2}$$

$$\delta = h\left[\left\{\frac{1+\left(1+\frac{\Delta z}{h}\right)^2}{2}\right\}^{1/3} - 1\right] \tag{3}$$

$$\tan(\phi+\phi_1) = \tan\phi + \gamma/(h+\delta) \quad , \tag{4}$$

$$\tan(\alpha+\alpha_1) = \{\gamma + (h+\delta)\tan\phi\}/(h-D+\delta) \quad , \tag{5}$$

$$l_1 = (h+\delta)/\cos(\phi+\phi_1) \quad , \tag{6}$$

$$l_2 = (h-D+\delta)/\cos(\alpha+\alpha_1) \quad . \tag{7}$$

The portions l_{1N} and l_{2N} of l_1 and l_2, respectively, are essential for consideration of extinction within the nebula. They are

$$l_{1N} = (h+H+\delta-D)/\cos(\phi+\phi_1) \tag{8}$$

$$l_{2N} = l_2 \quad . \tag{9}$$

The scattering angle at C'' is

$$\theta = \pi - (\phi+\phi_1) - (\alpha+\alpha_1) \quad . \tag{10}$$

2.2.2 IIb. $(h+\delta)<D$

Figure 1b depicts schematically the distances and angles for this configuration. The description is similar to case IIa. The analytical relations for h, δ, γ, l_1, l_{1N} and $(\phi+\phi_1)$ are the same as in case IIa but now they must be considered with reference to Figure 1b. The remaining equations are

$$\tan(\alpha-\alpha_1) \quad \{\gamma - (h-\delta)\tan\phi\}/(D-h-\delta) \quad , \tag{11}$$

$$l_2 = l_{2N} - (D-h-\delta)/\cos(\alpha+\alpha_1) \quad . \tag{12}$$

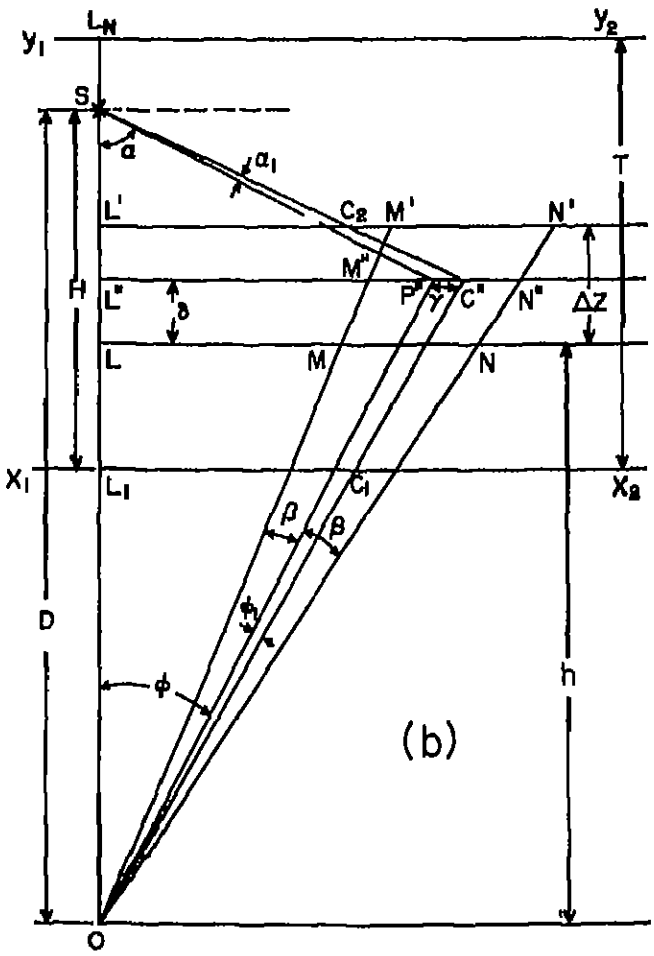

Fig. 1b. The same as in (1a) but here $h+\delta<D$.

2.3 Case III. Star in front of the nebula (SFN)

Figure 1c schematically represents the essential distances and angles. The relations for δ, γ, l_1, $(\alpha+\alpha_1)$ and $(\phi+\phi_1)$ are the same as in case IIa

once again, but must be taken with reference to Figure 1c. Further relations are

$$Z = (i-1)\Delta Z,\ i = 1, N, \quad (13)$$

$$h = D+H+Z, \quad (14)$$

$$I_{1N} = (Z+\delta)/\cos(\phi+\phi_1), \quad (15)$$

$$I_2 = (Z+H+\delta)/\cos(\alpha+\sigma_1), \quad (16)$$

$$I_{2N} = (Z+\delta)/\cos(\alpha+\sigma_1). \quad (17)$$

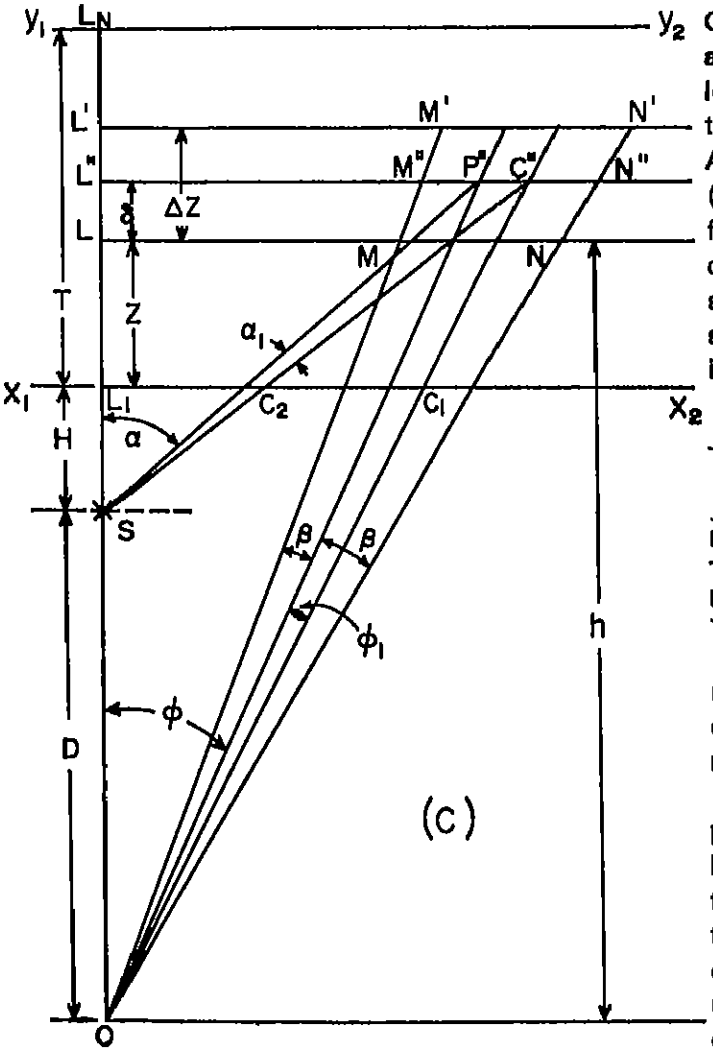

Fig. 1c. The schematic for the case of the reflection nebula with the star in the front (SFN).

The scattering angle at C'' in figure 1c is given by equation (10). The exact volume element MNN'M' in all the three cases turns out to be

$$\Delta V = h^2 \Delta Z \Delta\Omega \frac{\left\{1 + \frac{\Delta Z}{h} + \frac{1}{3}\left(\frac{\Delta Z}{h}\right)^2\right\}}{[\cos^2\phi - \sin^2\phi\tan^2\beta]^{3/2}} . \quad (18)$$

If $\beta \simeq 0°$ and $\left(\frac{\Delta Z}{h}\right) << 1$, this volume element approximates to the expression given by Greenberg and Roark (1967).

3. Results of Model Calculations

The values of geometrical parameters chosen on the basis of work by Greenberg and Hanner (1970) have been summarised in Table 1. The choice of size parameter (a_0) in the size distribution function of the type $n(a) \sim \exp[-5(a/a_0)^3]$ has been selected by keeping in view the best fits to observed interstellar extinction in the far-ultraviolet (see, for e.g. Greenberg and van de Hulst, 1973). We have adopted $a_0 = 0.3$ (0.1) 0.6 μm for ice. The wavelength dependent index of refraction of ice has been taken from Field *et al.* (1967) and Greenberg (1968). A useful tabulation has also been given by Shah (1967). The filter response function $Q_x(\lambda)$ in the far-ultraviolet bands have been used according to the data in Celescope Catalogue (Davis *et al.*, 1973). The stellar energy distribution for 23 Tau, the illuminating star for Merope reflection nebula, is chosen according to Andriesse *et al.* (1977).

Table 1. Geometrical Parameters

	Case I SBN	Case II SWN	Case III SFN
D (pcs)	160.0	126.0	126.0
T (pc)	1.0	1.0	1.0
H (pc)	1.25	0.25	0.04

The abscissae in all the subsequent figures represent the offset angle ϕ in minutes of arc. The dots correspond to the observations of the Merope reflection nebula obtained from satellite experiments (Andriesse *et al.*, 1977). Although observations on polarization in the far-ultraviolet are not available, we have included the theoretically calculated polarization for future comparison. The exact Mie theory of scattering by homogeneous smooth spheres (see, for e.g. van de Hulst, 1957; Shah, 1977c) has been used for all sizes and indices of refraction of the grains and for all wavelengths in the far-ultraviolet. The far-ultraviolet bands designated as U_1, U_2, U_3, U_4, have ranges of wavelengths (λ) 2150 to 3200, 1550 to 3150, 1350 to 2300, and 1050 to 2300, respectively. The colours and polarization given here have been obtained by integrating with respect to wavelength the intensity for each band in a manner analogous to that of Shah (1974).

3.1 *Surface brightness*

Figures 2, 3 and 4 for the three geometries SBN SWN and SFN respectively, show the nebular

intensities expressed in arbitrary units but normalized so that log S (λ, a_0, ϕ = 10') = 0, for all wavelengths and size parameters. This scheme allows one to compare model results directly with observations reduced in the same way. The set of curves a,b,c and d are plotted in each of these figures for wavelength λ = 1550 Å, 1800 Å, 2200 Å and 2500 Å, respectively. The solid curves are for the size parameter a_0 = 0.3μm and the dashed curves are for a_0 = 0.6μm. The theoretical values of log S, for the case of SWN vary most steeply at first for small

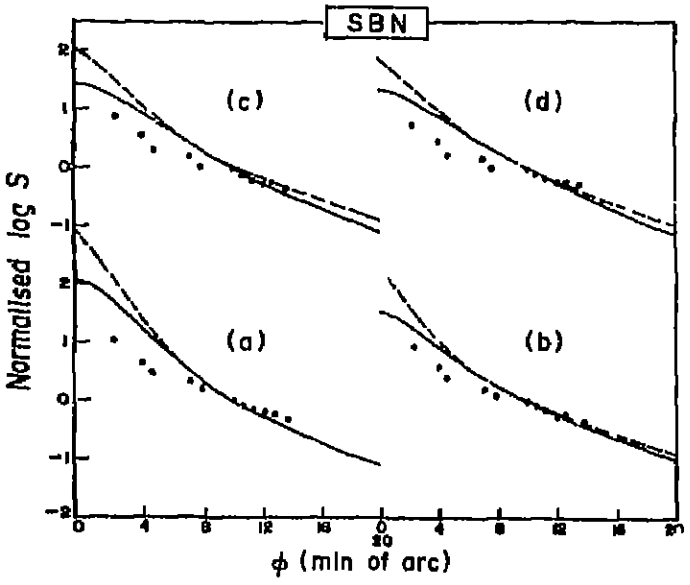

Fig. 2. The far-ultraviolet nebular surface brightness in arbitrary units but normalized such that log S (λ, a_0 ϕ = 10') = log S_{obs} (ϕ = 10') = 0. This is the case of SBN. The sets (a), (b), (c) and (d) correspond to wavelengths λ = 1550Å, 1800Å, 2200Å and 2500Å respectively. The ice grains have size parameter a_0 = 0.3 μm for—and 0.6 μm for - - -. The dots represent observations.

ϕ, the gradient being moderate for the case of SBN and much slower variation for log S occur for the case of SFN. The most suitable geometry for matching with the observations is found to be SFN for ice grains. This is clear from Figure 4 because for all the four wavelengths, the observational points lie close to the calculated models. However, the curves for widely separated values of a_0, *viz.*, a_0 = 0.1 and 0.6μm, are also closeby. Therefore, it is difficult to predict the size parameter precisely. For this, one must study the other observational features such as, for example, polarization. At present we have no data on polarization in the far-ultraviolet.

3.2 *Colours*

There are four ultraviolet bands designated U_1, U_2, U_3 and U_4 in the order of decreasing initial wave-

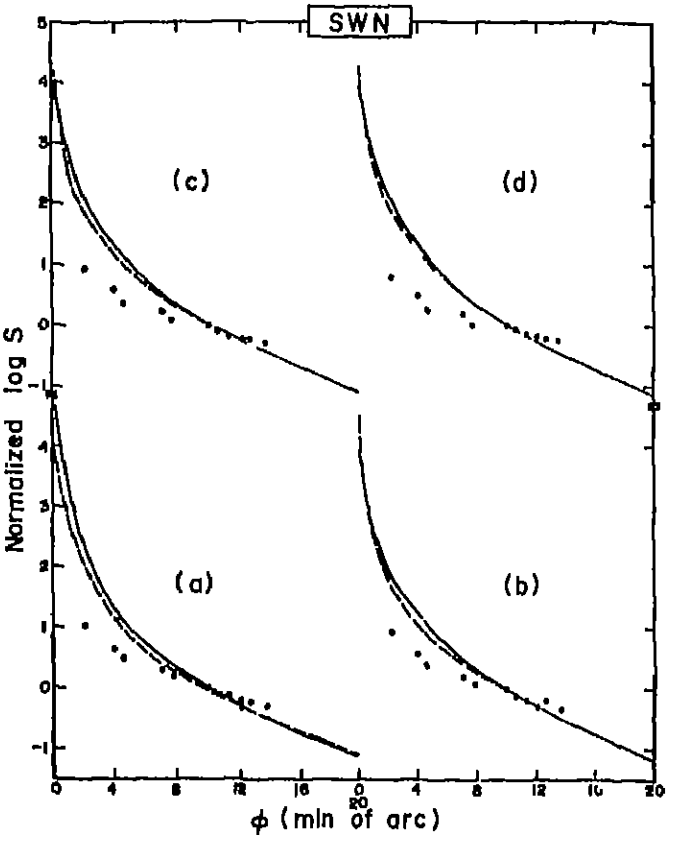

Fig. 3. The same as Figure 2 but for the case of SWN.

length as tabulated in Celescope Catalogue (Davis *et al.*, 1973). Following Greenberg and Roark (1967), the colour difference in magnitude for the first two bands is defined by

$$U_{21} = (U_2 - U_1)_* - (U_2 - U_1)_N$$

Thus U_{21} means the difference between the intrinsic $(U_2 - U_1)$ colour of the star and the $(U_2 - U_1)$ colour of the particular nebular region. The colour differences U_{32} and U_{13} are similarly defined. These

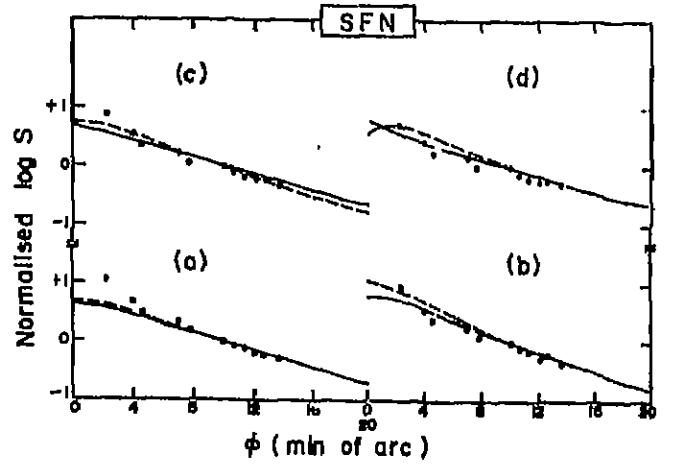

Fig. 4. The same as Figure 2 but for the case of SFN.

colours for the three cases of SBN, SWN and SFN are shown in Figures 5,6, and 7, respectively. As in the

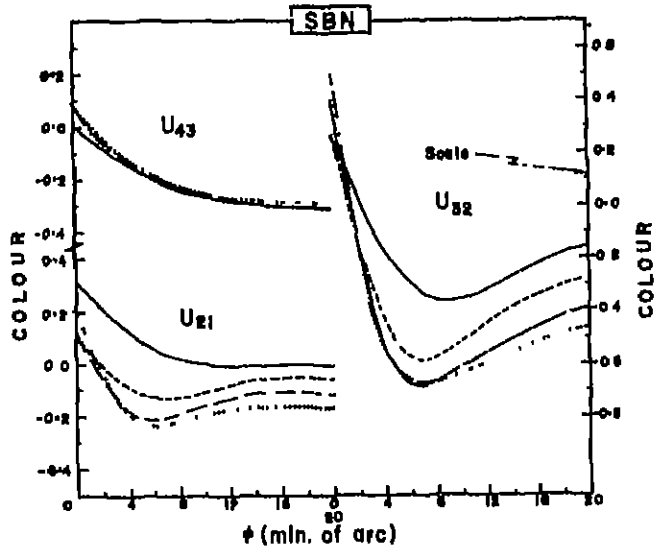

Fig. 5. The far-ultraviolet colour differences between two consecutive bands for star minus the same for reflection nebula. The star is behind nebula (SBN) The size parameter of the grains for each set of curves is a_0 - 0.3 μm for
0.4 μm for
0.5 μm for
0.6 μm for

case of UBV photometry, the nebula is relatively bluer in the vicinity of the star and redder with respect to the star after certain offset angle but the variation in colours is not necessarily monotonic. The U_{43} colour differences for various a_0 and for all the geometric cases lie close together. This is because the UV Filter response functions for U_1 and U_3 bands greatly overlap. The U_{21} colours in Figures 5 and 6 show a minimum almost for each a_0 chosen here. The nature

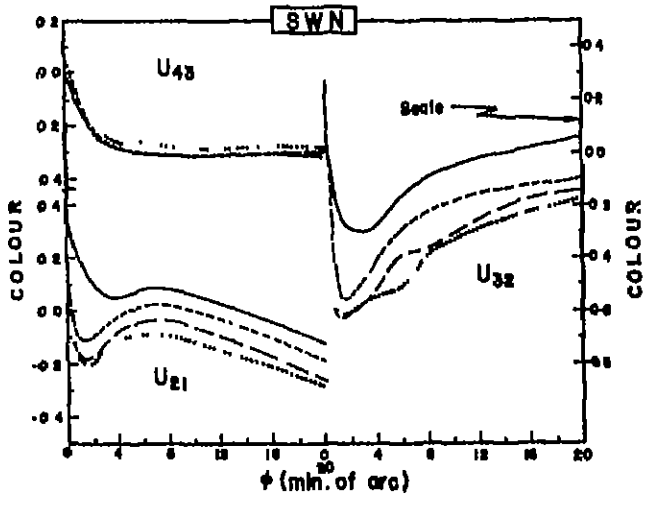

Fig. 6. The same as Figure 5 except for the case of SWN.

of these curves indicate that after minimum at certain offset angle, there is lesser reddening effect and possibly blueing effect can recur at an intermediate range of ϕ. For example, U_{21} colours for $a_0 = 0.4\mu$m (cf. Figure 6) are positive and thus nebula is bluer relative to the star in the range $5' \lesssim \phi \lesssim 10'$. The colours for the case of SFN in Figure 7 show a maximum near $\phi \sim 2'$ for $a_0 = 0.3\mu$m and 0.4μm. For other a_0, the colours vary monotonically. The reddening effect (*i.e.* negative colour difference) starts at much larger values of ϕ compared to other cases of SBN and SWN. The U_{32} colours in Figures 5 and 6 show only a minimum for each a_0. After exhibiting the reddening effect the U_{32} colours can become positive, as for instance for $a_0 = 0.3\mu$m in the case of SWN. The U_{32} colours for SFN, (Figure 7) also show the usual trends except for $a_0 = 0.3\mu$m which show the nebula bluer relative to the star for all $\phi \gtrsim 0.5'$.

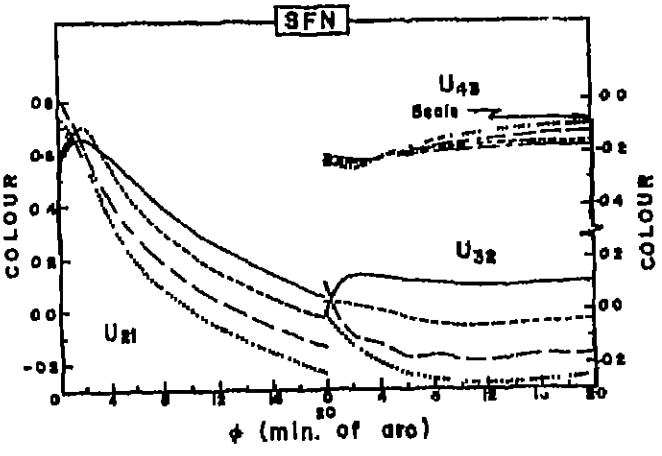

Fig. 7. The same as Figure 5 except for the case of SFN.

3.3 *Polarization*

Three sets of curves for degree of polarization of the nebular light as function of offset angle for the three geometric cases SBN, SWN, and SFN are displayed in Figures 8, 9 and 10, respectively. The sets (a), (b), (c) and (d) in each of these figures refer to bands U_1, U_2, U_3 and U_4, respectively. It may be noted that these results are for band integrated polarization. Although there are no observations on the far-ultraviolet polarization, we may note a few interesting points from the calculated models. In Figure 8, U_1 band polarization is negative for all offset angles considered and $a_0 \simeq 0.4$ to 0.6 μm; only for a_0 0.3 μm one has slightly positive polarization which reaches upto hardly 1.5% at ϕ 20'. For U_2 band, the polarization is negative

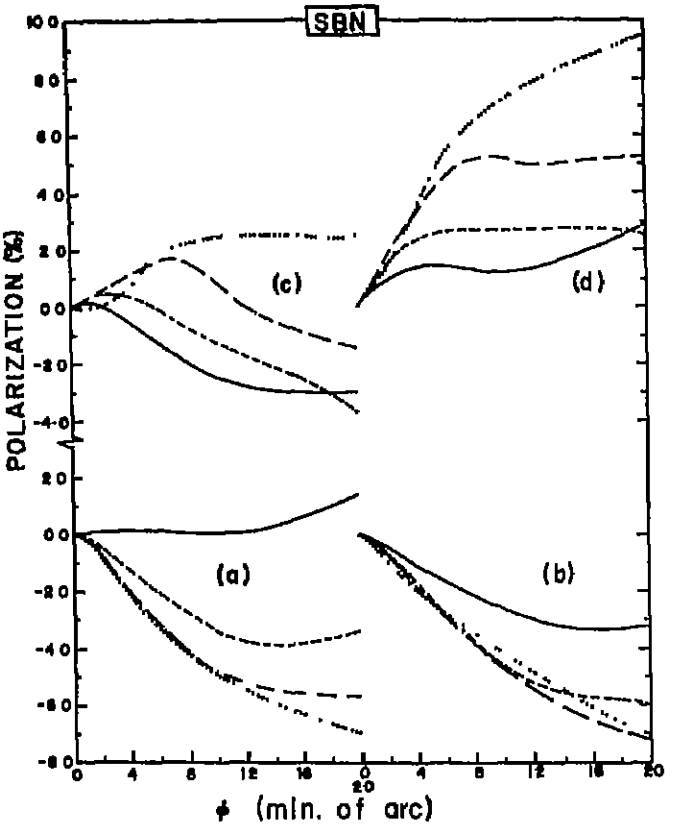

Fig. 8. The far-ultraviolet polarization from the model reflection nebula (SBN), as as given in Figure 5. The sets (a), (b), (c) and (d) correspond to the ultraviolet bands U_1, U_2, U_3, and U_4, respectively.

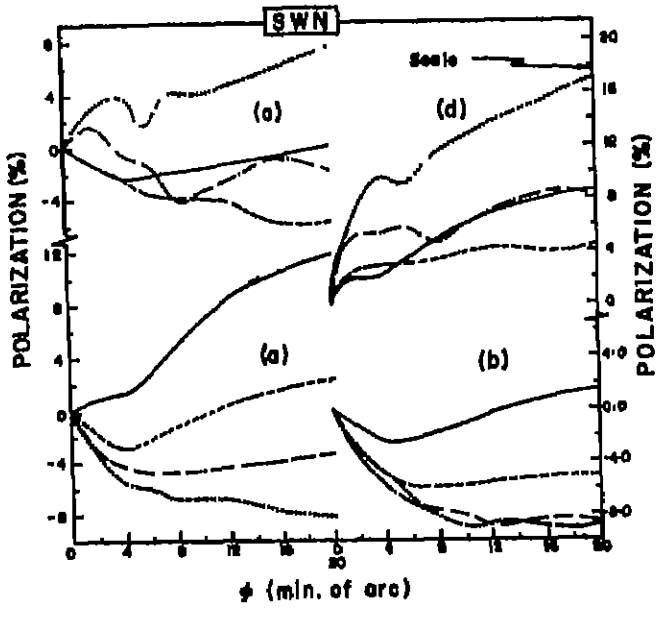

Fig. 9. The same as Figure 8 but the geometric case is SWN.

all the way upto $\phi = 20'$ for $a_o = 0.3$ (0.1) 0.6 μm. For band U_3, for each a_o, there is a distinct ϕ at which the polarization changes sign. For U_1 band (in Fig. 8), the polarization is positive for all ϕ and $a_o = 0.3$ (0.1) 0.6 μm. The absolute value of the degree of polarization is in general much smaller as compared to that in the UBV case. The cases of SWN and SFN also show certain individual characteristics for various bands and sizes. It is important to note that the curves for various sizes but for fixed band are well separated and carry imprint of geometric configuration of the nebula.

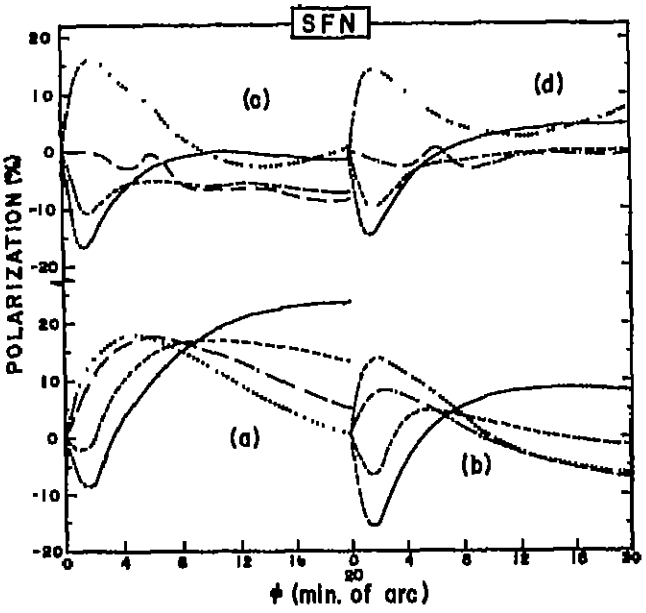

Fig. 10. The same as Figure 8 but the geometric case is SFN.

4. Discussion

The geometrical model of the reflection nebula in the form of the plane-parallel slab with the star in the front has shown some results on surface brightness which mimic the corresponding far-ultraviolet observations. This has been demonstrated here by using ice grains. Picking out the exact size parameter of the grains became difficult because of the crowding of the computed surface brightness curves for small and large values of the size parameter a_o in the size distribution function. The case of SWN with star very close to the front surface needs further consideration. The dielectric grains such as ice can satisfy the albedo requirement suggested by satellite observations (Andriesse *et al.*, 1977). These authors have been able to explain qualitatively certain observational features of the surface brightness by using models of plane-parallel slab and considering multiple scattering with Monte Carlo technique. They concluded that the phase function of the scattering particles changes

from a strongly forward scattering form at visual wavelength (5620 Å) to a more nearly isotropic form at far-ultraviolet wavelength (1550 Å). Such a trend in phase function must be understood from the viewpoint of the basic physics of electromagnetic scattering. Normally isotropic scattering is characteristic of Rayleigh scattering region which for moderate index of refraction occurs when $X \frac{2\pi a}{\lambda} << 1$; a size of the particle, λ the wavelength of light. As one proceeds towards geometric optics limit ($X >> 1$, *i.e.* larger particles and/or smaller wavelength as in the case of far-ultraviolet), the phase function at first is expected to attain more and more forward scattering form. As the parameter X becomes sufficiently large, the forward lobe fans out; here, back and side lobes may also show up. Ultimately in the extreme geometric optics limit when the particle presents itself as a mirror or wall, only the back scattering would prevail. One may refer to Born and Wolf (1970) for appropriate illustration of this statement. In fact, as one goes from visual to far-ultraviolet, that is in the direction of increasing X, the phase function would become increasingly anisotropic. This interpretation is consistent with the work of Greenberg and Hanner (1970) but not with the above-mentioned conclusions of Andriesse *et al.* (1977).

Polarization by spheres is not the only possible representation. However, they certainly reproduce adequately the degree of polarization, in the UBV and perhaps in the far-ultraviolet as well. Randomly oriented nonspherical particles cannot drastically change at least the general trends in the variation of polarization. However, in filaments in southern regions of Meropo nebula, there is some evidence of magnetically oriented nonspherical grains. This additional sophistication, not considered in the literature so far, needs to be studied in future models. Here we may note a few remarks by Greenberg (1977); (a) the case SFN is suspect because the back scattering ($\theta \geq 150°$) by nonspheres is substantially less than that from spheres, (b) the polarization and radiation scattered off of randomly aligned elongated particles is substantially greater than that from spheres.

The silicate and graphite have also been thought to be constituent materials of the grains in interstellar and circumstellar environments. Therefore, they need to be examined for their possible role in the phenomena of the reflection nebula.

In order to sort out the appropriate size and composition of the grains, it would be of great help to have additional data on polarization because the present results show this quantity to be very sensitive at least to the size parameter. Therefore, it is worthwhile to measure the polarization of the nebular light in a future space mission.

Acknowledgements

One of us (G.A.S.) wishes to thank Dr. M.K.V. Bappu for his encouragement. We are also grateful to Dr. J.M. Greenberg for his suggestions.

References

Aannestad, P. A., Purcell, E. M., 1973, *A. Rev. Astr. Astrophys.*, 11, 309.

Andriesse, C. D., Piersma, Th. R., Witt, A. N., 1977, *Astr Astrophys.*, 54, 841.

Bless, R. C., Savage, B. D., 1972, *Astrophys. J.*, 171, 293

Born, M., Wolf, E., 1970, *Principles of Optics*, Pergamon Press, Oxford

Davis, R. J., Deutschman, W. A., Hermandania, K. L., 1973, *Celescope Catalog of Ultraviolet Stellar Observations*, Smithsonian Institution, Washington.

Elvius, A., Hall, J. S., 1966, *Lowell Obs. Bull.*, 6, 257.

Field, G. B., Partridge, R. B., Sobel, H., 1967, *Interstellar Grains*, p 207, eds. J. M. Greenberg and T. P. Roark, NASA, SP-140.

Greenberg, J. M., 1968, *Nebulae and Interstellar Matter*, eds B. M. Middlehurst and L. H. Aller, Univ of Chicago Pr.

Greenberg, J. M., 1977, Private communication.

Greenberg, J. M., Hanner, M. S., 1970, *Astrophys. J.*, 161, 847.

Greenberg, J. M., Hong, S. S., 1974, *Galactic Radio Astronomy* p 155, eds. F. J. Kerr and S. C. Simonson, III, D. Reidel, Dordrecht.

Greenberg, J. M., Hulst, H. C., van de, eds. 1973, IAU Symp., 52.

Greenberg, J. M., Roark, T. P., 1967, *Astrophys. J.*, 147, 917.

Hulst, H. C., van de, 1957, *Light scattering by small particles*, John Wiley, New York.

Isobe, S., 1971, *Ann. Tokyo astr. Obs., Second Series*, 12, 263.

Isobe, S., 1975, *Ann. Tokyo astr. Obs.*, Second Series, 14, 141.

Jenkins, E. B., Savage, B. D., 1974, *Astrophys. J.*, 187, 243.

Jura, M., 1977, *Astrophys. J.*, 218, 749.

Kaplan, S. A., Pikelner, S. B., 1970, *The Interstellar Medium*, Harvard Univ. Press, Cambridge.

Krishna Swamy, K. S., O'Dell, C. R., 1967, *Astrophys. J.*, 147, 529.

Lillie, C. F., Witt., A. N., 1976, *Astrophys. J.* 208, 64.

Lilley, A. E., 1955, *Astrophys. J.*, 121, 559.

Nandy, K., Thompson, G. I., Jamar, C., Monfils, A., Wilson, R., 1975, *Astr Astrophys.*, 44, 195.

O'Dell, C. R., Hubbard, W. D., 1965, *Astrophys. J.*, 142, 591.

O'Dell, C. R., Hubbard, W. B., Peimbert, M., 1966, *Astrophys. J.*, 143, 743.

Peytremann, E., Davis, R.J., 1974, *Astrophys. J. Suppl.*, 28, 211.

Shah, G. A., 1967, *Ph. D. Thesis*, Rensselaer Polytechnic Institute, Troy, New York.

Shah, G. A., 1974, *Pramana*, 3, 336
Shah, G. A., 1977a, *Astr. Nachr.*, 298, 319
Shah, G. A., 1977b, *Pramana*, 9, 461
Shah, G. A., 1977c, *Kodaikanal Obs. Bull. Ser. A.*, 2, 42
Vanysek, V. Solc, M., 1973, I.A.U. Symposium No. 52
Watson, W. D., 1976, *Atomic and Molecular Physics and Interstellar Matter*, eds. R. Balian, P. Encrenaas, and J. Lequeux, North Holland, Amsterdam.